Scheme I

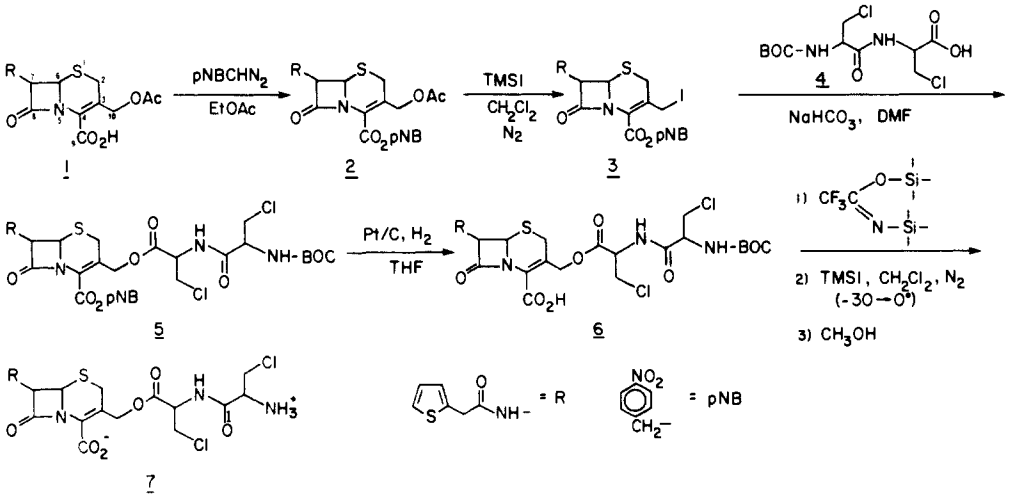

Table I. Susceptibility of Selected Microorganisms to Cephalosporin Dipeptidyl Esters

bacterial species	MIC, μg/mL[a] 7	8
Enterobacter aerogenes	100	>200
Enterobacter cloacae	14.1	>200
Escherichia coli JSR-O	14.1	>200
Escherichia coli JSR-O (Cl-Pep^R)[b]	>200	>200
Escherichia coli JSR-O (pBR322)[c]	7.05	>200
Escherichia coli (Ceph^R)[d]	7.05	>200
Staphylococcus aureus (Pen^R)[e]	0.85	>200
Corynebacterium JK	1.70	>200

[a] MIC = minimum inhibitory concentration. [b] This is an *E. coli* JSR-O strain selected for resistance to the dipeptide β-Cl-L-Ala-β-Cl-L-Ala (MIC >100 μg/mL).[11] [c] Contains the plasmid gene encoding for the TEM β-lactamase. [d] Resistant to cephalothin, I (MIC >200 μg/mL). [e] Resistant to penicillin G (MIC >200 μg/mL).

If the action of a periplasmic lactamase releases β-Cl-L-Ala-β-Cl-L-Ala in vivo,[16] as it does in vitro, this is likely to be only the first in a series of events that render **7** an antibiotic. Subsequent transformations are likely to include: (1) transport of the dipeptide across the inner plasmalemma, (2) hydrolysis of the peptide by a cytoplasmic peptidase, and (3) attendant inactivation by β-Cl-L-Ala[17] of alanine racemase, an enzyme essential for cell wall biosynthesis. Consistent with these expectations, exposure to β-Cl-L-Ala-β-Cl-L-Ala gives inactivation of alanine racemase in *E. coli* JSR-O; the loss of enzyme activity appears to require cleavage of the dipeptide by an aminopeptidase. We have also found that **7** leads to inactivation of the racemase in vitro, in a sequence that involves processing first of **7** by TEM β-lactamase and subsequent aminopeptidase hydrolysis of the liberated dipeptide.[18] We will provide later a more detailed account of the mechanism of action of this novel cephalosporin peptide ester.

Acknowledgment. We thank Carmen Torres for her work in obtaining the microbial susceptibility data. This research was supported in part by NIH Grant GM 29660 and by the Dow Chemical Co. We also acknowledge both the NIH (CA 14599, RR 01733) and the NSF (CHE 8206978, CHE 8312645) for funds allowing the purchase of NMR and mass spectrometry equipment.

Registry No. 1, 153-61-7; **2**, 41625-53-0; **3**, 100206-63-1; **4**, 100206-64-2; **5**, 100206-65-3; **6**, 100206-66-4; **7**, 100206-67-5; **8**, 100228-77-1; *N*-BOC-L-Ala-L-Ala, 27317-69-7; $pNBCHN_2$, 100206-68-6; β-lactamase, 9073-60-3.

(16) The mechanism of action of **7** in Gram-positive species may not be the same as that outlined for Gram-negative organisms. For example, the lactamases in Gram-positive bacteria are mostly extracellular.

(17) β-Chloroalanines are only weakly antibacterial, probably because they are poorly transported. Incorporation of the amino acid into a transportable peptide substantially increases its antibiotic potency (see ref 11).

(18) Cheung, K. S.; Mobashery, S.; Johnston, M., unpublished experiments.

Reactivity of $Cr(CO)_4$ in the Gas Phase

T. Rick Fletcher and Robert N. Rosenfeld*[1]

Department of Chemistry, University of California Davis, California 95616

Received May 29, 1985

Coordinatively unsaturated transition metals can affect the activation of alkanes[2] and the hydrogenation of olefins.[3] Pulsed lasers have been employed to generate such species and in studying the kinetics of their subsequent reactions.[4-6] Time-resolved infrared laser absorption methods provide a means to observe coordinatively unsaturated metal complexes, to characterize their vibrational spectroscopy and to directly determine their reaction kinetics.[4,5] Efforts toward understanding the chemistry of coordinatively unsaturated transition metals have focused primarily on the reactions of metal atoms[7] or monounsaturated metal complexes.[8] We report here new data on kinetics of association of a bisunsaturated complex, $Cr(CO)_4$, with a variety of ligands.

(1) Fellow of the Alfred P. Sloan Foundation (1985-1987).
(2) Janowicz, A. H.; Bergman, R. G. *J. Am. Chem. Soc.* **1982**, *104*, 352.
(3) Miller, M. E.; Grant, E. R. *J. Am. Chem. Soc.* **1984**, *106*, 4635.
(4) Fletcher, T. R.; Rosenfeld, R. N. *J. Am. Chem. Soc.* **1985**, *107*, 2203.
(5) Ouderkirk, A.; Wermer, P.; Schultz, N. L.; Weitz, E. *J. Am. Chem. Soc.* **1983**, *105*, 3354. Ouderkirk, A. J.; Weitz, E. *J. Chem. Phys.* **1983**, *79*, 1089.
(6) Welch, J. A.; Peters, K. S.; Vaida, V. *J. Am. Chem. Soc.* **1982**, *104*, 1089. Simon, J. D.; Peters, K. S. *Chem. Phys. Lett.* **1983**, *98*, 53.
(7) For example, see: (a) Jacobsen, D. B.; Freiser, B. S. *J. Am. Chem. Soc.* **1983**, *105*, 7487. (b) Houriet, R.; Halle, L. F.; Beauchamp, J. L. *Organometallics* **1983**, *2*, 1818.
(8) Seder, T. A.; Church, S. P.; Ouderkirk, A. J.; Weitz, E. *J. Am. Chem. Soc.* **1985**, *107*, 1432.

0002-7863/86/1508-1686$01.50/0 © 1986 American Chemical Society

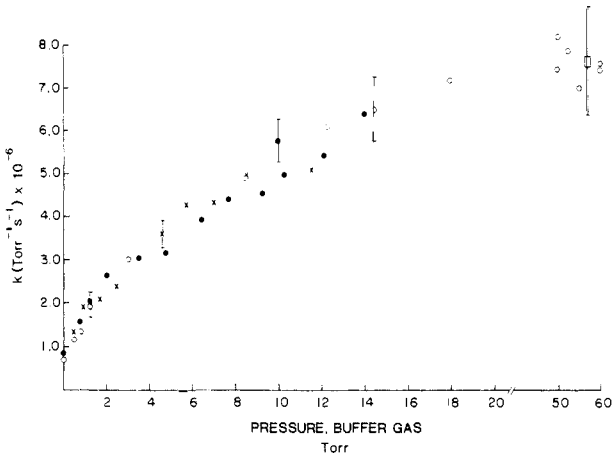

Figure 1. Observed rate constant for the recombination of $Cr(CO)_4$ with CO as a function of the bath gas pressure. The different symbols refer to data collected by using different probe laser frequencies (1915 or 1948 cm^{-1}) or bath gases (Ar or He). All data were obtained by using $p[Cr(CO)_6] = 0.015$ torr and $p[CO] = 0.400$ torr except (□) which is an independent measure of the high pressure rate constant made by holding bath gas pressure constant and varying $p[CO]$.

This data can provide a means of elucidating the relevant thermochemistry and mechanisms of such reactions as well as identifying structural and electronic effects which may be operative.

In our experiments,[4] $Cr(CO)_4$ is generated by the 249-nm pulsed-laser photolysis of $Cr(CO)_6$, eq 1. Samples consist of

$$Cr(CO)_6 \xrightarrow{249\ nm} Cr(CO)_4 + 2CO \qquad (1)$$

$Cr(CO)_6$ (0.010 torr), He, or Ar (0–80 torr) and a reactant, e.g., CO, H_2, NH_3, etc. (0.040–5.00 torr), and are contained in a 100-cm absorption cell. The time-dependent concentration of $Cr(CO)_4$ is monitored at either 1915 (b_2 CO stretch) or 1948 cm^{-1} (b_1 CO stretch), as previously described.[4,9] The temporal resolution of our detection system is ca. 10^{-7} s. $Cr(CO)_4$ is formed within 10^{-7} s of the photolysis of $Cr(CO)_6$ and is characterized by a simple exponential decay for at least 2.5 half-lives in all kinetic experiments. All data reported here were measured at ca. 300 K.

We have reinvestigated the kinetics of the recombination, eq 2. The apparent rate constant for this reaction increases with

$$Cr(CO)_4 + CO \xrightarrow[[He]]{k_2} Cr(CO)_5 \qquad (2)$$

[He] and approaches a limiting high pressure value of $k_2 = 7.5\ (\pm 1.3) \times 10^6$ $torr^{-1}$ s^{-1} (see Figure 1). The previously reported value[4] was not in the high pressure limit. The same pressure dependence is observed by monitoring $Cr(CO)_4$ at 1915 or 1948 cm^{-1}. This observation rules out any contribution from a D_{4h} structural isomer of $Cr(CO)_4$, as such a species must have only one infrared-active CO stretch. The observed pressure dependence of k_2 is consistent with a simple association mechanism, eq 3, where

$$Cr(CO)_4 + CO \underset{k_a}{\overset{k_c}{\rightleftharpoons}} [Cr(CO)_5]^* \xrightarrow{k_s[M]} Cr(CO)_5 \qquad (3)$$

the asterisk denotes ro-vibrational excitation and M represents the bath gas (He, Ar). When the steady-state approximation, $d[Cr(CO)_5]^*/dt = 0$, is made, the rate constant for $Cr(CO)_4$ decay is given by eq 4, which becomes independent of pressure only when

$$k_2 = k_c k_s[M]/(k_a + k_s[M]) \qquad (4)$$

$k_s >> k_a$. In this high pressure limit, we find k_2 to be approximately one-half the hard-sphere collision rate constant, $Z \approx 1.6 \times 10^7$ $torr^{-1}$ s^{-1}, indicating a small (≤0.5 kcal/mol) barrier to recombination.

(9) Burdett, J. K.; Graham, M. A.; Perutz, R. N.; Poliakoff, M.; Rest, A. J.; Turner, J. J.; Turner, R. F. *J. Am. Chem. Soc.* **1975**, *97*, 4805 and references therein.

Table I. High Pressure Limiting Rate Constants for Reaction 5

reactant, L	rate constant, $torr^{-1}$ s^{-1}	ionization potential of L, eV
$(CH_3)_2NH$	$1.5\ (\pm 0.2) \times 10^7$	8.24
NH_3	$1.1\ (\pm 0.2) \times 10^7$	10.20
C_2H_4	$9.1\ (\pm 1.4) \times 10^6$	10.50
CO	$7.5\ (\pm 1.5) \times 10^6$	14.00
H_2	$1.6\ (\pm 0.4) \times 10^6$	15.42
D_2	$1.6\ (\pm 0.4) \times 10^6$	15.47
Ar	no reaction[a]	15.8
He	no reaction[a]	24.48

[a] $k \leq 1 \times 10^4$ $torr^{-1}$ s^{-1}.

The pressure at which k_2 is half its high pressure limiting value defines $[M]_{1/2}$. From the data in Figure 1, $[M]_{1/2} \approx 5$ torr. Equation 4 indicates that $k_a = k_s[M]_{1/2}$. In separate experiments, we have determined $k_s \approx 3 \times 10^5$ $torr^{-1}$ s^{-1} when M = helium,[10] which gives $k_a \approx 1.5 \times 10^6$ s^{-1}. This result, in conjunction with an RRKM model[11] for k_a, can provide some insight regarding the bond dissociation energy,[10] $DH°[(CO)_4Cr\text{–}CO]$.

The kinetics of the reactions of $Cr(CO)_4$ with other ligands, L, eq 5, can also be determined by using laser absorption methods.

$$Cr(CO)_4 + L \rightarrow Cr(CO)_4L \qquad (5)$$

The kinetics of (5) were determined on the basis of measured $[Cr(CO)_4]$ lifetimes, since product spectra have not yet been characterized. In all cases, it was established that the rate of (5) varied linearly with [L]. Reported rate constants were obtained under high pressure limiting conditions ($p[He] \geq 50$ torr); see Table I.

Given the limited data available, it is unwarranted to draw too many conclusions at present; however, a few observations can be made. The data indicate that common ligands (R_3N, C_2H_4, CO) complex with $Cr(CO)_4$ within 1–2 gas kinetic collisions. It is interesting to note that the π-accepting ability[12] of the ligand appears to have little effect on the association rate (cf., NH_3, CO). There appears to be a qualitative correlation of reaction rate with the ligand's ionization potential (Table I), suggesting that the σ-donating ability of the ligand influences the association reaction. All of the reactive ligands listed in Table I possess σ-donating orbitals of a_1 symmetry as their highest occupied molecular orbital, while $Cr(CO)_4$ has an acceptor orbital of the same symmetry. A comparison of NH_3 with $(CH_3)_2NH$ suggests that steric effects are not significant for the latter system.

The reaction of $Cr(CO)_4$ with H_2 also occurs rapidly, ca. once in every ten gas kinetic collisions, indicating a barrier ≤ 1.5 kcal/mol. Thermochemical considerations allow metathetical reactions, (6) (R, R′ = H, D), to be ruled out as the mechanism

$$Cr(CO)_4 + R\text{–}R' \rightarrow Cr(CO)_4R + R' \qquad (6)$$

for $Cr(CO)_4$ decay. We conclude that an associative mechanism, (7), is operative, but our results do not address the question of

$$Cr(CO)_4 + R\text{–}R' \rightarrow Cr(CO)_4(RR') \qquad (7)$$

whether the product of (7) is best regarded as an oxidative adduct (negligible R–R′ interaction) or a complex where significant R–R′ bonding persists. We have measured the primary isotope effect to be $k_H/k_D = 1.0 \pm 0.2$. The lack of a measurable isotope effect suggests that the H–H (or D–D) bond is not strongly disrupted in the transition state for (7). While such data do not determine the structure of the association product, a recent matrix isolation study indicates that $Cr(CO)_4$ reacts with H_2 to yield a complex where appreciable H–H bonding persists,[13] a result also consistent with the observed kinetic isotope effect.

In conclusion, we find that $Cr(CO)_4$ associates with a variety of ligands with only a small activation barrier. Available data

(10) Fletcher, T. R.; Rosenfeld, R. N., manuscript in preparation.
(11) Robinson, P. J.; Holbrook, K. A. "Unimolecular Reactions"; Wiley-Interscience: New York, 1972.
(12) Cotton, F. A.; Wilkinson, G. "Advanced Inorganic Chemistry", 3rd ed.; Interscience: New York, 1972, p 720.
(13) Sweany, R. L. *J. Am. Chem. Soc.* **1985**, *107*, 2374.

suggest that the association rate is dominated by ligand to metal donor interactions. Further investigations on the origin of barriers to ligand addition and a comparison of the relative reactivity of $Cr(CO)_5$ and $Cr(CO)_4$ will be reported in a subsequent paper.[10]

Acknowledgment is made to the National Science Foundation (CHE-8500713) for support for this research.

Resolution and Structural Assignment of the Three Components in *trans*-1,2-Di(2-naphthyl)ethene Fluorescence[1]

J. Saltiel,*† D. F. Sears, Jr.,† F. B. Mallory,‡ C. W. Mallory,§ and C. A. Buser‡

Chemistry Departments, The Florida State University Tallahassee, Florida 32306
Bryn Mawr College, Bryn Mawr, Pennsylvania 19010
University of Pennsylvania Philadelphia, Pennsylvania 19104

Received November 7, 1985

The dependence of the 1,2-diarylethene fluorescence spectral shape on excitation wavelength, λ_{exc}, and other variables,[2] and fluorescence decay results requiring multiexponential fits[3] are attributed to the presence of equilibrating mixtures of aryl-rotational conformers. Electronic excitation reverses double- and single-bond character "freezing" ground-state conformers into noninterconverting populations of excited-state species exhibiting different intrinsic properties.[2,3] Pure component fluorescence spectra were obtained for *trans*-1-phenyl-2-(2-naphthyl)ethene, *t*-2-NPE, by application of principal component analysis (PCOMP), a curve resolution technique,[4] and structures were assigned by comparison with spectra from analogues.[5] We now report the application of the PCOMP/analogue approach to the resolution of three-component spectra using *trans*-1,2-di(2-naphthyl)ethene, DNE, and its conformationally restricted (steric hindrance) 3-methyl, MDNE, and 3,3′-dimethyl, DMDNE, derivatives.

Corrected fluorescence spectra of DNE, MDNE, and DMDNE ($\sim 10^{-5}$ M in methylcyclohexane, 30.0 °C) were measured as previously described,[5] except that the fluorimeter was interfaced to a CompuPro System 816 series microcomputer and digitized intensities were recorded at 1.0-nm increments. Changes in DNE fluorescence spectral shape with λ_{exc} and with $[O_2]$ agreed with earlier reports (Figure 1),[2,3] Subtle changes were observed for MDNE, but the fluorescence spectrum of DMDNE was insensitive to changes in λ_{exc} and $[O_2]$.

PCOMP analyses of emission spectra have been described.[5-7] Spectroexcitational emission input matrices (up to 150 × 150) were employed, each row of which represented a digitized, normalized fluorescence spectrum obtained at one of eight λ_{exc} in the presence or absence of O_2. Matrix columns differed by 1.0-nm increments spanning the fluorescence spectra. Recognition of significant eigenvectors was based on the magnitude of the eigenvalues. Both DNE and MDNE, treated separately, gave

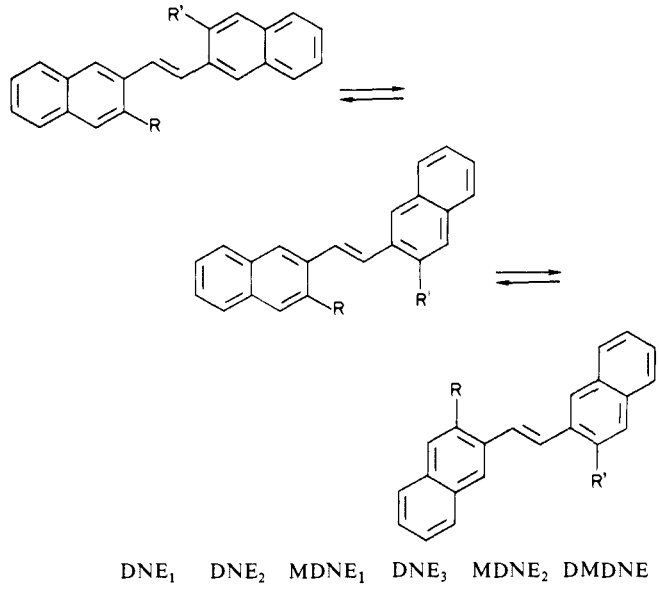

	DNE_1	DNE_2	$MDNE_1$	DNE_3	$MDNE_2$	DMDNE
R	H	H	H	H	H	CH_3
R′	H	H	CH_3	H	CH_3	CH_3
K_{sv}, M^{-1}	218 ± 33	90 ± 13	52 ± 16	90 ± 13	65 ± 2	52 ± 2

two-component solutions which accounted for >99% of the total variance of all measured spectra. In each case a vibronic structure was well resolved in the shorter wavelength component spectrum and much less so in the longer wavelength component spectrum; moreover, the fluorescence spectrum of DMDNE showed a better developed vibronic structure than the second MDNE component. In pursuing a three-component solution for DNE, it was assumed that (1) the longer wavelength DNE component spectrum is a combination of DNE_2 and DNE_3 fluorescence and (2) the subtle changes in the ratio of $MDNE_1/MDNE_2$ fluorescence in experimental spectra lead to poor estimates of the coefficients for the $MDNE_2$ fluorescence spectrum. The assumptions were tested by including the appropriately shifted DNE_2/DNE_3 composite solution spectrum and the DMDNE spectrum in the MDNE spectroexcitational matrix (see below). A two-component solution resulted with *eigenvectors nearly identical with those obtained for MDNE alone.* Thus, using MDNE and DMDNE fluorescence spectra to define the coefficients for resolved spectra for $MDNE_1$ and $MDNE_2$ allows separation of the broad DNE component spectrum into DNE_2 and DNE_3 contributions.[8] Finally, PCOMP was applied to a matrix of experimental spectra of DNE, MDNE (2-nm blue-shifted), and DMDNE (9-nm blue-shifted). The three pure component fluorescence spectra and the composite DNE_2/DNE_3 solution obtained when the DNE spectra are treated separately are shown in Figure 1. The three-component PCOMP solution gives a set of coefficients $(\alpha_i,\beta_i,\gamma_i)$ which define linear combinations of the eigenvectors $\mathbf{V}_\alpha$, $\mathbf{V}_\beta$, $\mathbf{V}_\gamma$ that represent best fit approximations of the experimental spectra, i.e., the spectrum corresponding to the ith row of the matrix is $\mathbf{S}_i = \alpha_i\mathbf{V} + \beta_i\mathbf{V} + \gamma_i\mathbf{V}$.[9] For a well-behaved solution, all points of a plot of the coefficients in Cartesian coordinates fall within a triangle whose edges represent coefficients for two-component mixtures and whose corners represent coefficients for the pure component spectra. Orthogonal and edge views of the triangle are shown in Figure 2. DNE points are clustered about a line representing a 55:45 DNE_2/DNE_3 ratio, hence the two-component solution when DNE spectra are treated alone and the essential role of the methyl derivative spectra in locating two corners of the triangle. Significantly, MDNE points are distributed about a 37:63 $MDNE_1/MDNE_2$ composition suggesting that the shift from the DNE_2/DNE_3 ratio reflects mainly the statistical factor of 2 (there

† The Florida State University.
‡ Bryn Mawr College.
§ University of Pennsylvania.

(1) Presented in part at the 33rd Southwest/37th Southeast Regional American Chemical Society Meeting, October 1985, Memphis, TN; Abstr. No. 307.

(2) For reviews, see: (a) Scheck, Y. B.; Kovalenko, N. P.; Alfimov, M. V. *J. Lumin.* **1977**, *15*, 157. (b) Fischer, E. *J. Photochem.* **1981**, *17*, 231. (c) Mazzucato, U. *Pure Appl. Chem.* **1982**, *54*, 1705.

(3) For key references, see: (a) Haas, E.; Fischer, G.; Fischer, E. *J. Phys. Chem.* **1978**, *82*, 1638. (b) Birks, J. B.; Bartocci, G.; Aloisi, G. G.; Dellonte, S.; Barigelleti, F. *Chem. Phys.* **1980**, *51*, 113.

(4) Lawton, W. H.; Sylvestre, E. A. *Technometrics* **1971**, *13*, 617.

(5) Saltiel, J.; Eaker, D. W. *J. Am. Chem. Soc.* **1984**, *106*, 7624.

(6) Warner, I. M.; Christian, G. D.; Davidson, E. R.; Callis, J. B. *Anal. Chem.* **1977**, *49*, 564.

(7) Aartsma, T. J.; Gouterman, M.; Jochum, C.; Kwiram, A. L.; Pepich, B. V.; Williams, L. D. *J. Am. Chem. Soc.* **1982**, *104*, 6278.

(8) 3-Methyl substitution on the naphthyl group of 2-NPE causes broadening of vibrational bands;[5] it is likely, therefore, that in an exact solution DNE_2 and DNE_3 spectra would have better resolved vibrational structure than the spectra of the methyl derivatives.

(9) See supplementary material.

0002-7863/86/1508-1688$01.50/0 © 1986 American Chemical Society